

Symmetry of high-piezoelectric Pb based complex perovskites at the morphotropic phase boundary

I. Neutron diffraction study on $\text{Pb}(\text{Zn}_{1/3}\text{Nb}_{2/3})\text{O}_3$ -9% PbTiO_3

Yoshiaki UESU^{1,2,*}, Masaaki MATSUDA³, Yasusada YAMADA^{2,3}, Kouji FUJISHIRO⁴, Dave E. COX⁵, Beatriz NOHEDA⁵ and Gen SHIRANE⁵

¹*Department of Physics, Waseda University, 3-4-1 Okubo, Shinjuku-ku, Tokyo 169-8555, Japan*

²*Advanced Research Institute, Waseda University, 3-4-1 Okubo, Shinjuku-ku, Tokyo 169-8555, Japan*

³*Advanced Science Research Center, Japan Atomic Energy Research Institute, Tokai, Ibaraki 319-1195, Japan*

⁴*Materials and Structures Laboratory, Tokyo Institute of Technology, 4259 Nagatsuda, Midori-ku, Yokohama 226-8503, Japan*

⁵*Department of Physics, Brookhaven National Laboratory, Upton, New York 11973, USA*

(Received October 24, 2018)

The symmetry was examined using neutron diffraction method on $\text{Pb}(\text{Zn}_{1/3}\text{Nb}_{2/3})\text{O}_3$ -9% PbTiO_3 (PZN/9PT) which has a composition at the morphotropic phase boundary between $\text{Pb}(\text{Zn}_{1/3}\text{Nb}_{2/3})\text{O}_3$ and PbTiO_3 . The results were compared with those of other specimens with same composition but with different prehistory. The equilibrium state of all examined specimens is not the mixture of rhombohedral and tetragonal phases of the end members but exists in a new polarization rotation line $M_c^\#$ (orthorhombic-monoclinic line). Among examined specimens, one exhibited tetragonal symmetry at room temperature but recovered monoclinic phase after a cooling and heating cycle.

KEYWORDS: Piezoelectricity, ferroelectricity, morphotropic phase boundary, neutron diffraction, $\text{Pb}(\text{Zn}_{1/3}\text{Nb}_{2/3})\text{O}_3$ -9% PbTiO_3

§1. Introduction

Extremely high piezoelectricity was found near the morphotropic phase boundary (MPB) of mixture compounds of Pb-based complex perovskite oxides and PbTiO_3 .¹⁾ Examples are 92% $\text{Pb}(\text{Zn}_{1/3}\text{Nb}_{2/3})\text{O}_3$ -8% PbTiO_3 ,²⁾ 52% PbZrO_3 -48% PbTiO_3 ³⁾ and 65% $\text{Pb}(\text{Mg}_{1/3}\text{Nb}_{2/3})\text{O}_3$ -35% PbTiO_3 .¹⁾ Hereafter they are abbreviated as PZN- x PT, PZT x and PMN- x PT with composition ratio x (%) of PbTiO_3 . In fact the electromechanical coupling coefficient k_{33} exceeds 90% at the MPB where a strain up to 1.7% can be induced by an electric field. Furthermore some materials exhibit low hysteresis strain-field curve. These properties have attracted much attention to the piezoelectric applications, i.e., energy-conserving transformation of electric and mechanical energy into one another in medical diagnostic apparatus, actuators, high power ultrasonic transducers, underwater acoustic and so on.

The origin of ultra-high piezoelectricity at the MPB of these materials has been puzzling for long time. However recent two approaches promoted a better understanding of the phenomenon: One is the first-principle study by Fu and Cohen.⁴⁾ Under the assumption that a large piezoelectricity is driven by polarization rotation induced by an electric field, they calculated the most favorable path in BaTiO_3 , which is similar to the high-piezoelectric complex systems. Observed strain-field relation was quantitatively explained by choosing a path

where polarization rotates between two extremities of rhombohedral [111] and tetragonal [001] axes in the monoclinic plane (M_a). Later the existence of monoclinic phases was proved to be compatible with the Devonshire theory by introducing higher order term P^8 which reflects strong unharmonicity of the system.⁵⁾ The first principle calculation also showed that the high-piezoelectricity is induced due to the existence of a monoclinic phase.⁶⁾

Another approach to the origin of high-piezoelectricity is experimental. Noheda et al. examined precisely crystal symmetries at a very narrow region of the MPB of PZT48, and found that the PZT48 shows monoclinic structure with the point group C_m with polarization vector lying in the monoclinic plane M_a .⁷⁻¹⁰⁾ They also performed measurements on PZN-8PT samples and found that PZN-8PT has rhombohedral symmetry in as-grown state but an orthorhombic phase is irreversibly induced by the electric field.¹¹⁾ It indicates that examined samples are in the proximity of a rhombohedral-orthorhombic boundary in the phase diagram. In fact, recent high-resolution synchrotron X-ray diffraction study by Cox et al. revealed that a PZN-9PT powder sample (9PT-2) prepared carefully from a poled single crystal shows an orthorhombic symmetry.¹²⁾ Orthorhombic phase is another extremity in polarization rotation path (M_c) connecting [001] to [101] as shown in Fig. 1. In this case, the polarization possibly rotates within the (010) monoclinic plane of the point group P_m under the external electric along the [001] direction. As a necessary condition for high-piezoelectricity is the existence of monoclinic phase,^{4,5)} PZN-9PT would exhibit

* E-mail: uesu93@mn.waseda.ac.jp

also a monoclinic phase depending on the history of sample treatment. For this motivation, we examined four PZN-9PT samples including 9PT-2 in order to determine the symmetry at the MPB of PZN-PT system. In particular, measurements of two samples (9PT-4 and 9PT-5) were performed using neutron diffraction method.

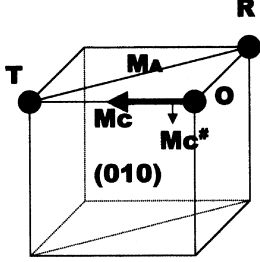


Fig. 1. Possible polarization rotation paths in high-piezoelectric complex compounds at the morphotropic phase boundary. T, O and R indicate the polarization directions in tetragonal, orthorhombic and rhombohedral phases, respectively. M_A and M_C are polarization rotation paths in monoclinic $(1\bar{1}0)$ and (010) planes, respectively. $M_C^\#$ is a new polarization rotation path found in PZN/9PT.

§2. Experimental conditions

PZN-9PT single crystals were grown by a flux method.¹³⁾ Four samples were prepared with different sample prehistory. Among them 9PT-1 is single crystal plates cut from same as-grown single crystal, 9PT-2 a powder sample prepared from a poled single crystal, 9PT-4 a (001) plate which has been once exposed to the electric field, and 9PT-5 a (001) plate which has never experienced the field, similar to 9PT-1, but cut from a different single crystal.

Neutron diffraction measurements were performed on 9PT-4 and 5 using triple-axis spectrometers TAS1 and TAS2 installed in JRR-3M in Japan Atomic Energy Research Institute. For the measurements, the horizontal collimator sequences were $20'-20'-S-20'-20'$ with $E_i=13.64\text{meV}$ ($\lambda=2.449\text{\AA}$) on TAS1 and $20'-20'-S-20'-10'$ with $E_i=13.72\text{meV}$ ($\lambda=2.441\text{\AA}$) on TAS2. Diffraction profiles of 9PT-5 were measured by a mesh-scanning method in the $\{001\}^*$ plane at room temperature, 10K, 80K and 200K. Measurements of 9PT-4 and of after-cooling profiles of 9PT-5 were performed by a simple scanning method.

§3. Results and discussions

3.1 Neutron diffraction study on 9PT-5

Diffraction profiles in $(hk0)$ and $(h0l)$ planes were measured at room temperature. Fig. 2 shows those around 200 (a) and 020 (b) reciprocal points observed in the $(hk0)$ plane. Here the ordinate and abscissa are referred to the cubic axes and the lattice point with $h(k)=2$ corresponds to $Q=3.116\text{\AA}^{-1}$. Several peaks are observed and can be interpreted as a juxtaposition of tetragonal domain configurations, which are indicated in Fig. 3(a). Seven domains T_i ($i=1$ to 7) existed in an irradiated part of the sample. In particular, from the locations of T_1

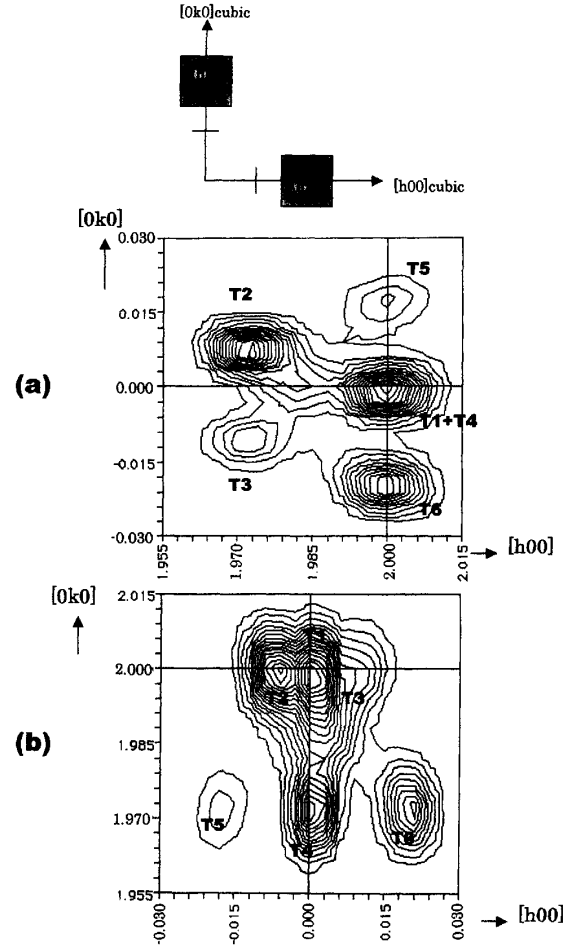


Fig. 2. Neutron diffraction profiles at room temperature around 020 reciprocal point in the $(hk0)$ (a) and 200 in the $(h0l)$ planes of 9PT-5. They are a juxtaposition of tetragonal domain configurations T_i ($i=1$ to 7) as shown in Fig. 3(a). The referred axes are those of cubic phase, and the lattice point with $h(\text{or } k)=2$ corresponds to $Q=3.116\text{\AA}^{-1}$. The upper figure shows scanning areas of the present experiment.

and T_4 , tetragonal lattice parameters were determined as $a=c=4.033\text{\AA}$, $b=4.085\text{\AA}$. These values coincide well with those of 9PT-1, which is a mixture of orthorhombic and tetragonal phases, as will be discussed later.

The tetragonal phase could appear even at room temperature as a quenched high-temperature phase. Therefore if the sample is cooled down to a low temperature, it would be transformed into the ground state, which would be maintained after heating. In this expectation, we performed low temperature measurements with same sample and similar diffraction geometry. Fig. 3 shows diffraction profiles observed at 10K. Measurements were made around same reciprocal points as in Fig. 2. Here (a) indicates those around 020 and (b) 200 both in the $(hk0)$ plane. Contrary to the profiles at room temperature, main peaks are interpreted by monoclinic domains. A small portion of tetragonal domains still exist in low temperature but with a marked diminution of intensities, e.g., that of T_6 . Three types of mono-

Table I. Lattice parameters of 9PT-1, 2, 4 and 5.

	9PT-1	9PT-2	9PT-4	9PT-5		
Single crystal or powder	Single crystal	Powder ^{a,12)}	Single crystal	Single crystal		
Prehistory of field application	No	Yes	Yes	No		
Temperature	RT	RT	RT	RT ^b	10K	RT ^c
Symmetry	O + T	O	O	T	M ^d + T	M + T
Lattice parameters	O: a=4.059 b=4.036 c=4.059 $\beta_o=90.15$ T: a=4.0317 b=4.0317 c=4.0840	a=4.0623 b=4.0328 c=4.0623 $\beta_o=90.15$	a=4.062 b=4.033 c=4.062 $\beta_o=90.15$	a=4.033 b=4.033 c=4.085	M: a=4.051 b=4.019 c=4.067 $\beta=90.19$ T: a=4.019 b=4.019 c=4.090	M: a=4.052 b=4.028 c=4.057 $\beta=90.11$ T: a=4.028 b=4.028 c=4.078
Experimental method	X-ray	SR	Neutron	Neutron		

^aPrepared from a poled single crystal. ^bBefore cooling. ^cAfter cooling. ^dM is dominant.

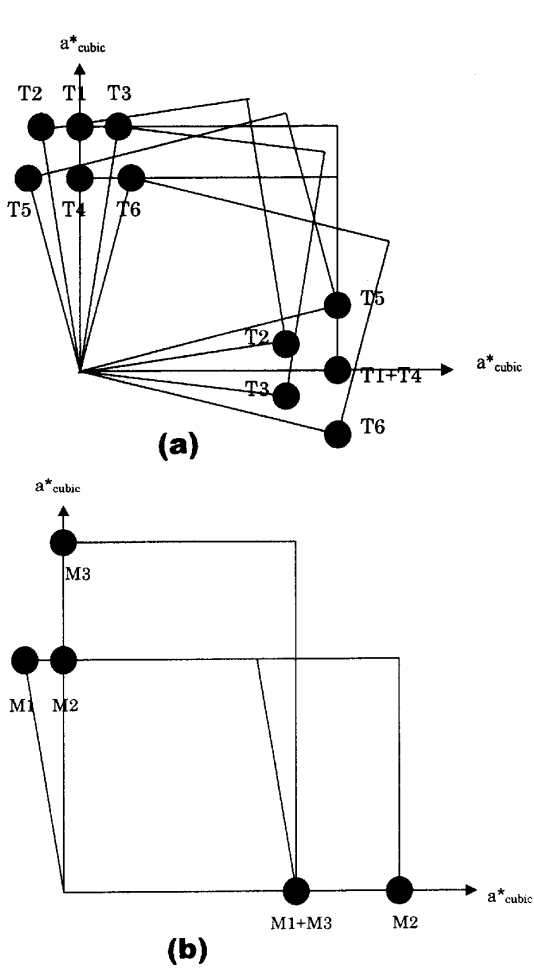


Fig. 3. (a) indicates tetragonal domain configuration corresponding to the observed pattern in Fig. 2, and (b) monoclinic one corresponding to Fig. 4. Solid circles represent lattice points of these domains

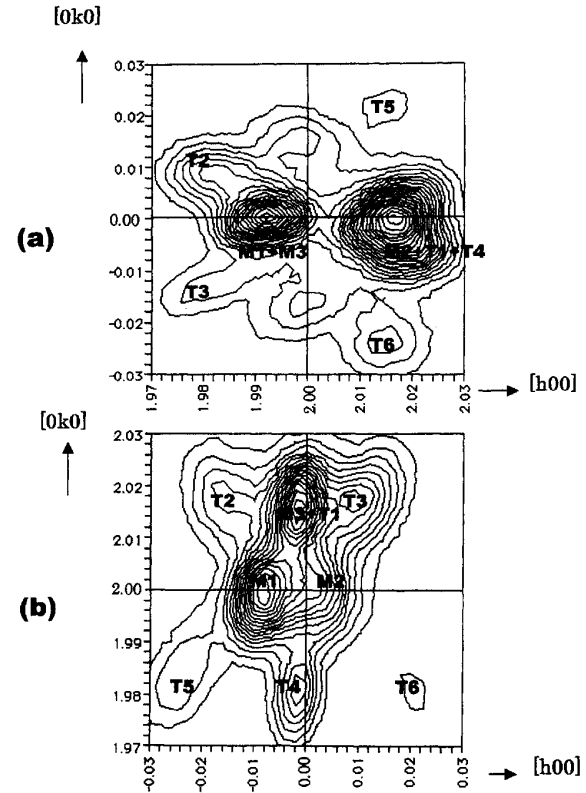


Fig. 4. Neutron diffraction profiles at 10K around 020 (a) and 200 (b) reciprocal points in the $(hk0)$ plane of 9PT-5. M_1 , M_2 and M_3 indicate corresponding monoclinic domains in Fig. 3(b). The referred axes are those of cubic and the lattice point $h=2$ on the $[h00]$ axis corresponds to $Q=3.102\text{\AA}^{-1}$, and $k=2$ on the $[0k0]$ axis to $Q=3.090\text{\AA}^{-1}$.

clonic domain M_1 , M_2 and M_3 contribute to the profiles as shown in Fig. 4. Lattice parameters were determined as $a=4.051\text{\AA}$, $b=4.019\text{\AA}$, $c=4.067\text{\AA}$, $\beta=90.19^\circ$ in monoclinic phase, and $a=b=4.019\text{\AA}$, $c=4.090\text{\AA}$ in tetrag-

onal phase. Similar measurements were performed at 80K, 200K and room temperature in this sequence. Essentially similar profiles were observed at these temperatures and the monoclinic symmetry is maintained in higher temperature. Lattice parameters determined at 10K and RT are tabulated in Table I, and their temperature dependences are shown in Fig. 5(a) for axial angle β and (b) for lattice constants, where those of 9PT-1 and 2 are shown for comparison. Here β means a monoclinic axial angle between a_m and c_m as shown in the upper figure of Fig. 5(a). When $a_m=c_m$, the crystal system becomes orthorhombic with a_o and c_o which are perpendicular to each other (Fig. 5(a)). However, the monoclinic

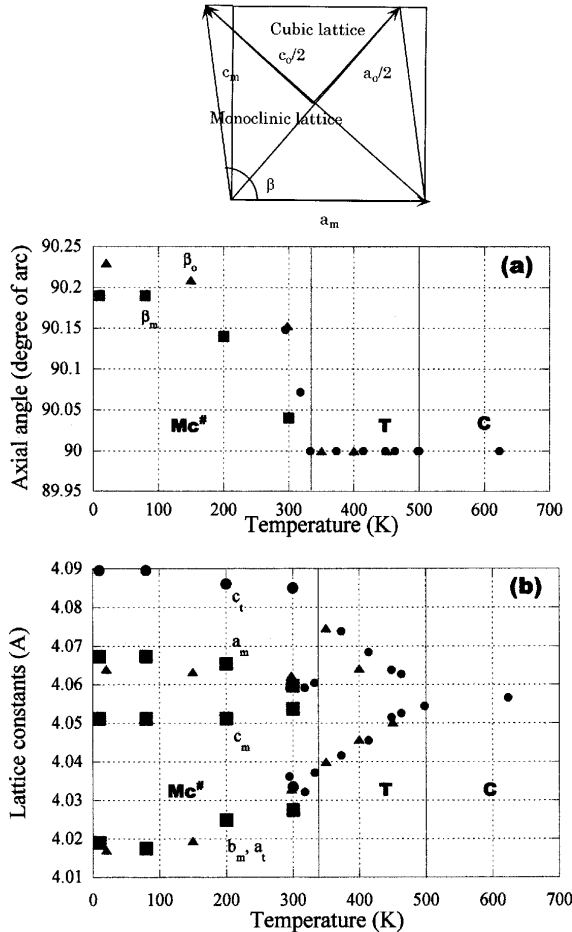


Fig. 5. Temperature dependences of monoclinic lattice parameters a_m , b_m , c_m and β_m of 9PT-5. Orthorhombic lattice parameters $a_o=c_o$, b_o and β_o of 9PT-1 and 2¹⁵⁾ are shown for comparison. The axes are referred to the cubic ones. (a) indicates axial angles β , and (b) lattice constants a, b and c . Here red squares indicate monoclinic lattice parameters a_m , b_m , c_m , β_m of 9PT-5, blue circles tetragonal lattice parameters $a_t=b_t$, c_t of 9PT-5, violet triangles of 9PT-2, and solid circles of 9PT-1.

axes are chosen in Table I and Fig. 5, β of the orthorhombic limit being indicated by β_o . The monoclinic lattice parameters vary with temperature almost in same manner as orthorhombic ones. This means that the observed monoclinic state is located near the orthorhombic limit in the (010) plane (Fig. 1).

3.2 Re-examination of the symmetry of 9PT-1

On the procedure of systematic analyses of the symmetry of PZN/9PT, we noticed that the previously published data of 9PT-1¹⁴⁾ should be re-examined. θ - 2θ scanning profiles were measured using (111) and (100) plates in temperature range from 300 to 625K by a high-accuracy X-ray diffractometer in SPMS, Ecole Centrale Paris. (222) and (400) profiles were shown in Fig. 6. They have been analyzed under an assumption that rhombohedral and tetragonal phases co-exist below the ferroelectric phase transition at 500K. In this analysis, tetragonal lattice constants a , b , c and rhombohedral $a(=b=c)$ were determined independently from the (100) plate and (111) plate experiments, respectively. However, we encountered a discrepancy when we tried to explain the (400) profile by the mixture of tetragonal and rhombohedral reflections which were determined from the (222) reflection as shown in Fig. 6(a). In particular, the peak around $2\theta=86.6^\circ$ cannot be explained by the model. The problem could be solved when orthorhombic symmetry is considered to be true in place of rhombohedral one (Fig. 6(b)). The determined lattice constants coincide well with those of 9PT-2.

3.3 Comparison of four 9PT samples

We also determined lattice parameters of 9PT-4 by neutron diffraction method by simple scanning along $[h00]$ and $[0k0]$ directions. 9PT-4 is a (001) single crystal plate, which has been under the electric field of maximum 10kV/cm. It was found that the symmetry of 9PT-4 is orthorhombic with same lattice parameters as 9PT-2.

The lattice parameters of 9PT-1, 2, 4, and 5 are tabulated in Table I, and their temperature dependences are shown in Fig. 5. These results indicate clearly that the ground state of PZN/9PT, the morphotropic phase boundary compound between PZN and ferroelectric PT, is orthorhombic $Amm2$ (9PT-1, 2, 4) with spontaneous polarization along the $[101]$ axis or monoclinic Pm with polarization vector lying in the (010) plane (9PT-5). The space group in orthorhombic state is $Amm2$ with P_s along the $[011]$ direction, similar to the orthorhombic phase in $BaTiO_3$,¹²⁾ while that of the monoclinic phase is Pm judging from the domain configuration shown in Fig. 3(b) and 4, and the fact that monoclinic lattice constants are smoothly connected with those of orthorhombic constants with increasing temperature from 10K. The reason of this difference of symmetry could be explained by a slight change of composition ratio of PT to PZN, or by the existence of small local field due to internal stress, impurity, etc, as the energy surface near the symmetric orthorhombic axis is expected to be flat (see the part II of the paper).¹⁵⁾

In conclusion, the thermal equilibrium state of PZN/9PT at room temperature is not the mixture of rhombohedral and tetragonal phases of end members of pure PZN and PT, but orthorhombic or monoclinic single phase. This symmetry-lowering at the MPB has been already found in PZT48 and PZN-8PT, and the present result confirms that the phenomenon is quite common in Pb-based MPB compounds. However, it should be stressed that the present study disclosed a new po-

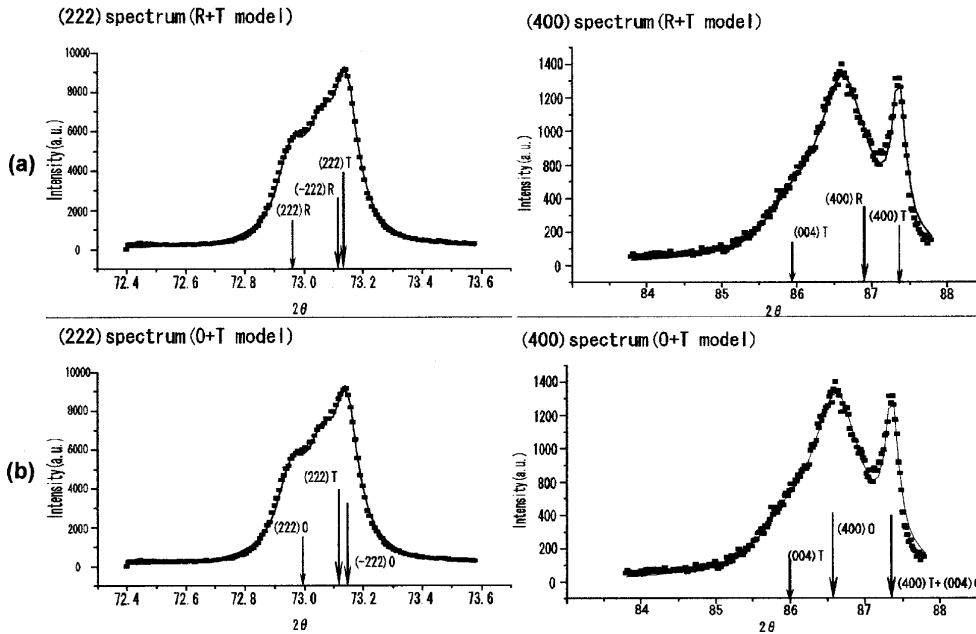


Fig. 6. Diffraction profiles of (222) and (400) reflections of 9PT-1 measured by X-ray diffraction method ($\text{CuK}\beta$, $\lambda=1.3922\text{\AA}$). Lines indicate expected diffraction positions of rhombohedral-tetragonal mixture model(upper figure), and of orthorhombic-tetragonal mixture model(lower figure).

larization rotation path $M_c^\#$ (orthorhombic-monoclinic-tetragonal) in PZN-9PT, which is different from M_a in PZT48 and $R-M_a-M_c$ in PZN-8PT.¹⁶ It was also found that the intrinsic symmetry at the MPB could be obtained after an on-off cycle of electric field along the [001] direction, or a cooling-heating cycle.

A theoretical treatment of the present results is described in Part II of the paper.¹⁵

Acknowledgements

We are grateful to Dr. Y. Yamashita, R & D center of Toshiba Co., for providing us PZN/9PT samples, and Dr. J. M. Kiat, SPMS, Ecole Centrale Paris, for his cooperation in X-ray diffraction experiment of 9PT-1.

Financial supports of Grant-In-Aid for Science Research from Monbu-Kagakusho, Grant for Development of New Technology from Shigaku-Shinkozaidan, Waseda University Grant for Special Research Projects and US DOE under contract No.AC0298CH10866 are also gratefully acknowledged. This work was performed under US-Japan Cooperative Neutron Research Program.

84 (2000) 5427.

- 7) B. Noheda, D. E. Cox, G. Shirane, E. Cross and S-E. Park: Appl. Phys. Lett. **74** (1999) 2059.
- 8) B. Noheda, J. A. Gonzalo, E. Cross, R. Guo, S-E. Park, D. E. Cox and G. Shirane: Phys. Rev. B **61** (1999) 8687.
- 9) R. Guo, E. Cross, S-E. Cross, B. Noheda, D. E. Cox and G. Shirane: Phys. Rev. Lett. **84** (2000) 5423.
- 10) B. Noheda, D. E. Cox, G. Shirane, R. Guo, B. Jones and E. Cross: Phys. Rev. B **63** (2001) 14103.
- 11) B. Noheda, D. E. Cox, G. Shirane, S-E. Park, E. Cross and Z. Zhong: Phys. Rev. Lett. **86** (2001) 3891.
- 12) D. E. Cox, B. Noheda, G. Shirane, Y. Uesu, K. Fujishiro and Y. Yamada: Appl. Phys. Lett. (9th issue of July, 2001 in press).
- 13) M. L. Mulvihill, S-E. Park, G. Risch, Z. Li, K. Uchino and T. R. Shroud: Jpn. J. Appl. Phys. **35** (1996) 3984.
- 14) Y. Uesu, Y. Yamada, K. Fujishiro, H. Tazawa, S. Enokido, J. M. Kiat and B. Dkhil: Ferroelectrics **217** (1998) 319.
- 15) Y. Yamada, Y. Uesu, M. Matsuda, K. Fujishiro, D. E. Cox, B. Noheda and G. Shirane: This issue.
- 16) K. Ohwada, K. Hirota, P. W. Rehrig, P. M. Gehring, B. Noheda, Y. Fujii, S-E. Park and G. Shirane: J. Phys. Soc. Japan (condense matter #0105086) (submitted).

1) S-E. Park and T. R. Shroud: J. Appl. Phys. **82** (1997) 1804.

2) J. Kuwata, K. Uchino and S. Nomura: Ferroelectrics **37** (1981) 579.

3) B. Jaffe, W. R. Cook, H. Jaffe: *Piezoelectric Ceramics* (Academic Press, London, 1971).

4) H. Fu and R. E. Cohen: Nature **403** (2000) 281.

5) D. Vanderbilt and M. H. Cohen: Phys. Rev. B **63** (2001) 94108.

6) L. Bellaiche, A. Garcia and D. Vanderbilt: Phys. Rev. Lett.